

# Lifetime Plots of $N$ and $\Delta$ Resonances

N. G. Kelkar<sup>1</sup>, M. Nowakowski<sup>2</sup>, K. P. Khemchandani<sup>1</sup> and Sudhir R. Jain<sup>1</sup>

<sup>1</sup>*Nuclear Physics Division, Bhabha Atomic Research Centre,  
Mumbai 400 085, India*

<sup>2</sup>*Universität Dortmund, Institut für Physik, D-44221 Dortmund, Germany*

## Abstract

We present a method for the determination of baryon resonances and their parameters using existing relations between the  $S$ -matrix and time delay in pion nucleon scattering. We draw attention to the fact that the existence of a positive maximum in time delay, which is related to the lifetime of a resonance is a necessary criterion for the existence of a resonance and should be used as a constraint in conventional analyses which locate resonances from poles of the  $S$ -matrix and Argand diagrams. The usefulness of the time delay or lifetime plots of resonances is demonstrated through a detailed analysis of the time delay in several partial waves of  $\pi N$  elastic scattering.

PACS numbers: 14.20.Gk, 13.85.Dz, 03.65.Nk

## 1 Introduction

There seem to be several views in literature regarding the definition and characterization of a resonance. In a review article [1], Dalitz has discussed various criteria for the existence of a resonance elaborately with the conclusion that for the case of a pole in the  $S$ -matrix,  $S(E)$ , in the unphysical  $E$ -plane lying sufficiently close to the physical  $E$  axis, there is no ambiguity in the conclusion of the existence of a resonance. However, the authors in Ref. [2] studied the correspondence between resonances and  $S$ -matrix poles and constructed examples in such a way that a sharp resonance was produced without an accompanying pole in the unphysical sheet. They noted that even the inverse correspondence, namely, (pole of the  $S$ -matrix on the unphysical sheet)  $\rightarrow$  (unstable particle) may be questioned. Another alternative would be to locate resonances from relative maxima in the scattering cross sections. However, as pointed out in Ref. [3], peaks in cross section cannot be a conclusive evidence of resonances.

To identify the baryon resonances, for example, one studies the meson-baryon scattering data. Using partial wave techniques for the analysis, the energy-dependent scattering amplitude (or the  $T$ -matrix) is obtained by fitting the cross section data. Resonances are then determined by locating the poles of the  $T$ -matrix on the unphysical sheet and studying the Argand diagrams of the complex  $T$ -matrix. Due to model dependence in the analyses of the energy-dependent amplitudes, there are differences in the resonance parameters quoted by different groups [4]. The resonance receiving confirmation from several analyses is considered to be well established.

In contrast to these conventional analyses, we demonstrate a method of obtaining the resonance parameters based on existing relations between the collision times and scattering matrix. We make use of the most fundamental requirement stated in literature and text books [5], that the formation of a resonance should introduce a large positive time delay in the scattering of particles. This is indeed an appealing concept as it confirms our intuition that the formation of an unstable intermediate on-shell state in a scattering process should be accompanied by a positive time delay. We extract resonance parameters from the energy distribution of time delay. Though in principle, the non-resonant background can deform the positive resonant structure in the vicinity of a resonance, we would still expect some positive region around the resonance point with, perhaps a less dominant peak. In general, this is confirmed by our study.

Starting with the definition of time delay in terms of the  $S$ -matrix, we obtain its relation with the  $T$ -matrix and scattering phase shifts. We shall first demonstrate the validity of the method with examples of well-known  $N$  and  $\Delta$  resonances. Later on we proceed to the analysis of time delay in various partial waves of  $\pi N$  elastic scattering using the available single energy values as well as some energy-dependent forms of the  $T$ -matrix. Before we move on to the discussion of time delay, it is important to note that the *time delay plots* of the present work are *not* the same as the *speed plots* [6] which have been wrongly popularized as time delay plots in literature. Speed plots are positive definite by definition. Time delay plots can also assume negative values and only a positive peak signals a resonance. A discussion on this issue can be found in Ref. [7].

In passing, we note that time delay has recently been revived in the form of a related concept in quantum mechanics called arrival time which is then mostly used in tunneling processes [8]. Further, time delay has also been

used to obtain the density of resonances [9].

## 2 Time delay and scattering phase shifts

In the early fifties, using a wave packet analysis, it was shown by Bohm [10], Eisenbud [11] and Wigner [12], that the time delay  $\Delta t$  in binary collisions can be defined in terms of the energy derivative of the scattering phase shift as follows:

$$\Delta t = 2\hbar \frac{d\delta}{dE}. \quad (1)$$

The formation of a resonance, which occurs as an unstable, intermediate state in a scattering process, introduces a time delay between the arrival of the incident wave packet and its departure from the collision region. Hence a positive maximum in the energy derivative of the phase shifts was expected at energies around the resonance. For a rigorous definition in classical and quantum scattering theory, see [13].

The connection between the lifetime matrix and scattering phase shifts was later established by Smith [14]. The point of view taken in deriving the lifetime matrix  $\mathbf{Q}$  was that a lifetime, or delay time can be associated with every collision. If the interaction between particles, and, the initial conditions of the collision, like energy and angular momentum are known, it is possible to compute the “time” the particles spend within any distance  $R$  of each other. To get a definition independent of  $R$ , the lifetime in Ref. [14] was defined as the difference between the time that the particles spend within a distance  $R$ , with and without the interaction, in the limit  $R \rightarrow \infty$ . As a function of energy,  $\mathbf{Q}$  was shown to be related to the scattering matrix  $\mathbf{S}$ :

$$\mathbf{Q} = -i\hbar \mathbf{S} \frac{d\mathbf{S}^\dagger}{dE}. \quad (2)$$

The time delay for a particle injected in the  $i^{th}$  channel and emerging in the  $j^{th}$  channel is then given by

$$\Delta t_{ij} = \text{Re} \left[ -i\hbar (S_{ij})^{-1} \frac{dS_{ij}}{dE} \right]. \quad (3)$$

From Eq. (3) we see that, in the case of purely elastic scattering, and, using

a phase shift formulation for the  $S$ -matrix where  $S = e^{2i\delta}$ , we get,

$$\Delta t_{ii} = 2\hbar \frac{d\delta}{dE} \quad (4)$$

which is exactly the relation mentioned in Eq. (1) between time delay and scattering phase shift. These  $\Delta t_{ii}$  are the lifetimes of metastable states or resonances in elastic scattering. At high energies, where apart from elastic scattering the possibility of scattering into inelastic channels also opens up, the  $S$ -matrix is defined as  $S = \eta e^{2i\delta}$ , where  $\eta$  is the inelasticity parameter defined such that  $0 \leq \eta \leq 1$ . By substituting the modified  $S$  in Eq. (3) it can be seen that the expression for  $\Delta t_{ii}$  for elastic scattering in the presence of inelastic channels remains unchanged from that for purely elastic scattering.

It is clear from the above expressions that the time delay can also take negative values resulting from phase shifts which are decreasing as a function of energy. However, the negative lifetimes cannot assume arbitrarily large values. As shown by Wigner [12], the causality condition puts a constraint on the lower value of the time delay as,

$$\Delta t = 2\hbar \frac{d\delta}{dE} > -a \quad (5)$$

where  $a$ , which is the radius of the scattering centre can be interpreted as the range of the interaction potential. A rapidly decreasing phase shift would lead to a large negative value of  $\Delta t$ . A large negative value of  $\Delta t$  corresponds to a large time advancement and hence means that the outgoing particle has left the scattering centre even before the incident one arrived. Such a situation violates causality and hence a limit as given by Wigner appears on the minimum value of time delay. The implications of negative time delay or time advancement, which we do observe in some regions of  $\pi N$  elastic scattering will be discussed later in Section 5.

### 3 Time delay and $T$ -matrix

Let us start by defining the average time delay for a particle injected in the  $i^{th}$  channel (assuming that it has a probability  $|S_{ij}|^2$  of emerging into the  $j^{th}$  channel) as,

$$\langle \Delta t_i \rangle_{av} = \sum_j S_{ij}^* S_{ij} \Delta t_{ij} \quad (6)$$

Separating the contributions of the elastic and inelastic channels, we get,

$$\langle \Delta t_i \rangle_{av} = \eta^2 \Delta t_{ii} + \sum_{j \neq i} S_{ij}^* S_{ij} \Delta t_{ij}. \quad (7)$$

Thus we see that, in the absence of inelastic channels (i.e. when the resonance formed from the  $i^{th}$  channel decays with a 100% branching fraction into the  $i^{th}$  channel)  $\Delta t_{ii}$  gives the full lifetime of the resonance, while in general, in the presence of inelastic channels, the time delay  $\Delta t_{ii}$  is associated with the partial lifetime of a multichannel resonance which decays back to the channel from which it originated.

Instead of using the phase shift formulation of the  $S$ -matrix, we now start by defining the  $S$ -matrix in terms of the  $T$ -matrix, i.e.,

$$S = 1 + 2iT, \quad (8)$$

as is usually done in partial wave analyses of resonances [15, 16]. The matrix  $T$  contains the entire information of the resonant and non-resonant scattering and is complex ( $T = T^R + iT^I$ ). Now, substituting for  $\Delta t_{ij}$  from Eq. (3) into Eq. (6) for the average time delay, we get,

$$\langle \Delta t_i \rangle_{av} = Re \left[ -i\hbar \sum_j (S_{ij})^* \frac{dS_{ij}}{dE} \right]. \quad (9)$$

On substituting Eq. (8),

$$\langle \Delta t_i \rangle_{av} = \sum_j 2\hbar \left[ \frac{dT_{ij}^R}{dE} + 2T_{ij}^R \frac{dT_{ij}^I}{dE} - 2T_{ij}^I \frac{dT_{ij}^R}{dE} \right]. \quad (10)$$

From the above equation, we see that in addition to the possibility of evaluating time delay from the scattering phase shifts, we can also evaluate it using an energy-dependent amplitude  $T$ . The time delay  $\Delta t_{ii}$ , in terms of the real and imaginary parts of the amplitude  $T$  is given as,

$$S_{ii}^* S_{ii} \Delta t_{ii} = 2\hbar \left[ \frac{dT_{ii}^R}{dE} + 2T_{ii}^R \frac{dT_{ii}^I}{dE} - 2T_{ii}^I \frac{dT_{ii}^R}{dE} \right], \quad (11)$$

where  $S_{ii}^* S_{ii}$  can be evaluated using Eq. (8). In the present work, we have evaluated the time delay in  $\pi N$  elastic scattering and hence,  $i$  corresponds to  $\pi N$  in the above equation.

## 4 Time delay and wave packets

For completeness and a better understanding of the concept of time delay, we will briefly discuss two aspects related to time delay. The first one has to do with the well-known fact that survival probability and therefore also lifetime of an unstable quantum state depends on its preparation. Explicit formulae including this wave packet can be found, for instance for unstable neutral kaons, in Ref. [17]. We would expect that a similar dependence should also be present in time delay. This is indeed the case and the exact expression for time delay as given in Ref. [18] is,

$$\Delta t = 8\pi^2\hbar \int_0^\infty dE |A(E)|^2 2 \frac{d\delta}{dE}, \quad (12)$$

where  $A(E)$  is the initial wave packet in momentum space. If the wave packet is sharply centered around an energy  $E_0$ , we recover equation (1) as  $\Delta t(E_0)$ . Strictly speaking, equations (1), (11) and (12) represent a time delay due to interaction. One can also calculate the average time spent by a particle within a sphere of radius  $r$  which maybe interpreted as interaction range  $a$  when  $r \sim a$  (see Eq. (5)). Taking the two concepts together, i.e. time delay and the the average time spent within a scatterer (not including interaction) one can derive an expression [18]

$$T(a) = 8\pi^2\hbar \int_0^\infty dE |A(E)|^2 \left\{ 2 \frac{d\delta}{dE} + 2a - \frac{\sin[2(\delta + ka)]}{k} \right\} \quad (13)$$

which is usually interpreted as the time spent within the interaction region of radius  $a$  in the presence of interaction. Since Eq. (13) can be rewritten as an integral over a probability,  $T(a)$  is always positive definite in contrast to (1), (11) and (12). We emphasize again that negative regions of time delay due to interaction are not unphysical, only constrained by Wigner's causality relation (5).

In the applications of time delay to  $\pi N$  scattering in the next section, we will not make use of the formulae (12) and (13). We will assume, as it is customary in particle physics, that the wave packets are sufficiently sharp in energy to justify the usage of equations (1) and (11). Moreover, however useful the expression (13) might be, it does not represent the time delay in scattering which is related to the lifetime of a resonance.

Table 1: Resonance parameters taken from the Summary Table [4]

$L_{2I,2J}$	Mass (MeV)	Width (MeV)	Fraction of decay to $\pi N$ mode	Partial Width (MeV)
$P_{33}$	1230 to 1234	115 to 125	99%	
$D_{13}$	1515 to 1530	110 to 135	50 to 60%	55 to 81

In the next Section, we shall evaluate the time delay in several partial waves of  $\pi N$  elastic scattering. We have checked that the values of time delay,  $\Delta t_{ii}$ , obtained either using the derivative of the real phase shifts as in Eq. (4) or the  $T$ -matrix as in Eq. (11) are the same. Since both the methods are equivalent, one can in fact use fits to the single energy values [19] of phase shifts to extract resonance parameters.

## 5 Lifetimes Plots of resonances in $\pi N$ elastic scattering

We now turn to the analysis of the existing pion nucleon scattering data using lifetime plots. To demonstrate the validity of the method, we plot the lifetime of two well-known baryon resonances. In Fig. 1 are shown the real and imaginary parts of the complex  $T$ -matrices, the phase shifts and the corresponding time delay in the  $P_{33}$  and  $D_{13}$  partial waves in  $\pi N$  scattering, evaluated using the  $T$ -matrices (solid lines) which fit the single energy values of  $T$  very well. The filled circles in Fig. 1 are the single energy values of phase shifts extracted from the cross section data on  $\pi N$  elastic scattering [20]. The widths of the  $P_{33}$  and  $D_{13}$  peaks at half maximum can be read from Fig. 1 to be around 116 and 50 MeV respectively. The peaks in their lifetime distributions occur at 1216 and 1512 MeV respectively. The parameters of these resonances, as listed by the Summary Table (ST) of the Particle Data Group [4], are tabulated in Table 1. These parameters are determined assuming a Breit-Wigner form of the energy distribution. The values of the widths  $\Gamma$ , listed in the ST correspond to the lifetime  $\Delta t(E)$  at the resonance energy  $E_R$ . If we write a Breit-Wigner form for the lifetime

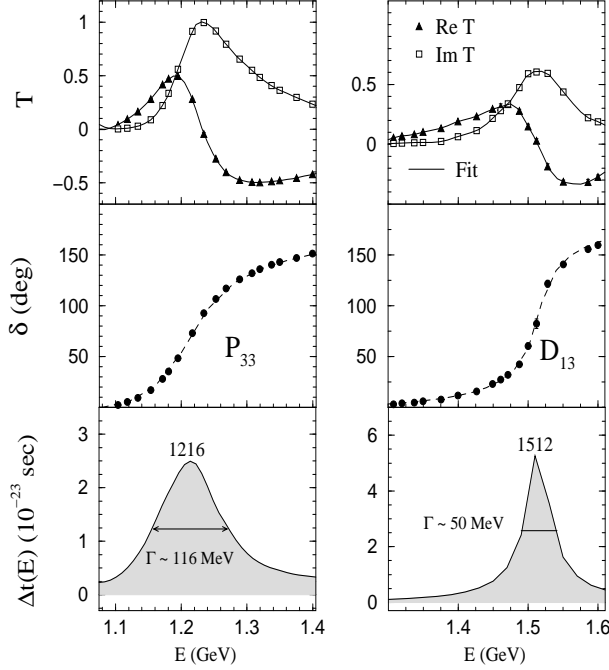


Figure 1: Single energy values of the real part of the  $T$ -matrix (filled triangles), imaginary part of  $T$  (open squares), phase shifts (filled circles) and the time delay  $\Delta t$  evaluated in the  $P_{33}$  and  $D_{13}$  partial waves of  $\pi N$  elastic scattering. The time delay is evaluated using the  $T$ -matrix given by the solid lines which fit the single energy values very well.

distribution as follows:

$$\Delta t(E)_{BW} = \frac{\hbar\Gamma}{(E_R - E)^2 + \frac{1}{4}\Gamma^2} \quad (14)$$

then the lifetime at the resonance energy  $E_R$  is

$$\Delta t(E_R)_{BW} = \frac{4\hbar}{\Gamma}. \quad (15)$$

To compare with the parameters of the ST given in Table 1, we use the above equation and find that the widths of the two resonances, namely, the  $P_{33}$  and  $D_{13}$  in Fig. 1, for a Breit-Wigner energy distribution are around 108 and 50 MeV respectively. These values are in fairly good agreement

with those in Table 1. In case of  $\Delta(1232)$  which has 99% fraction of its decay to the  $\pi N$  mode, the  $\Delta t(E)$  plot gives the full width of this resonance. In the case of the  $D_{13}$  resonance, however, the width corresponds to the partial width for the  $\pi N$  decay channel. Thus we see that in the case of purely elastic scattering as well as in the case of elastic scattering in the presence of inelastic channels, the method is reliable. This method provides a straightforward means of extracting resonance parameters, since the peak position and width of the time delay distribution give the mass and width of the resonance, respectively. A comment on non-resonant background is in order here. It was noted by Höhler [21] that the non-resonant background shifts the conventional resonance parameters from the pole values. Since the time delay plots of the present work contain both the resonant as well as non-resonant background contributions, we expect the peaks in time delay and their widths to be shifted from the pole positions. This is indeed the case for the  $P_{33}$  resonance above, which as noted in Ref. [21] does have a large background.

## 5.1 Time delay from energy-dependent amplitudes

One of the standard methods of determining resonances is to perform a partial wave analysis of the available scattering data to obtain the energy-dependent amplitudes and locate its poles on the unphysical sheet to extract the resonance parameters. If these poles correspond to resonances, one would expect to see a positive maximum in time delay at the energies where the poles occur. However, none of the existing analyses are constrained by this necessary condition. In what follows, we use the energy-dependent solutions obtained from the SAID program [20] as an example of such analyses, to evaluate the time delay. We start with the  $I = 1/2$  partial waves in  $\pi N$  elastic scattering. In Fig. 2a we plot the SAID solution FA02 of the complex amplitudes. The corresponding time delay, using these  $T$ -matrices and those from an earlier analysis (SM95 solutions) by the same group, is plotted in Fig. 2b. The two solutions in general, give rise to similar values of time delay in most partial waves except for the  $P_{11}$  and  $P_{13}$ , where the peak positions are changed. The newer solutions FA02 are in better agreement with the single energy values and the prominent peak around 2 GeV in  $P_{11}$ , seen with the SM95 calculation is not seen with FA02. We observe the resonant peaks in the  $P_{11}$ ,  $S_{11}$ ,  $D_{13}$ ,  $D_{15}$ ,  $F_{15}$  and  $P_{13}$  partial waves close to the pole

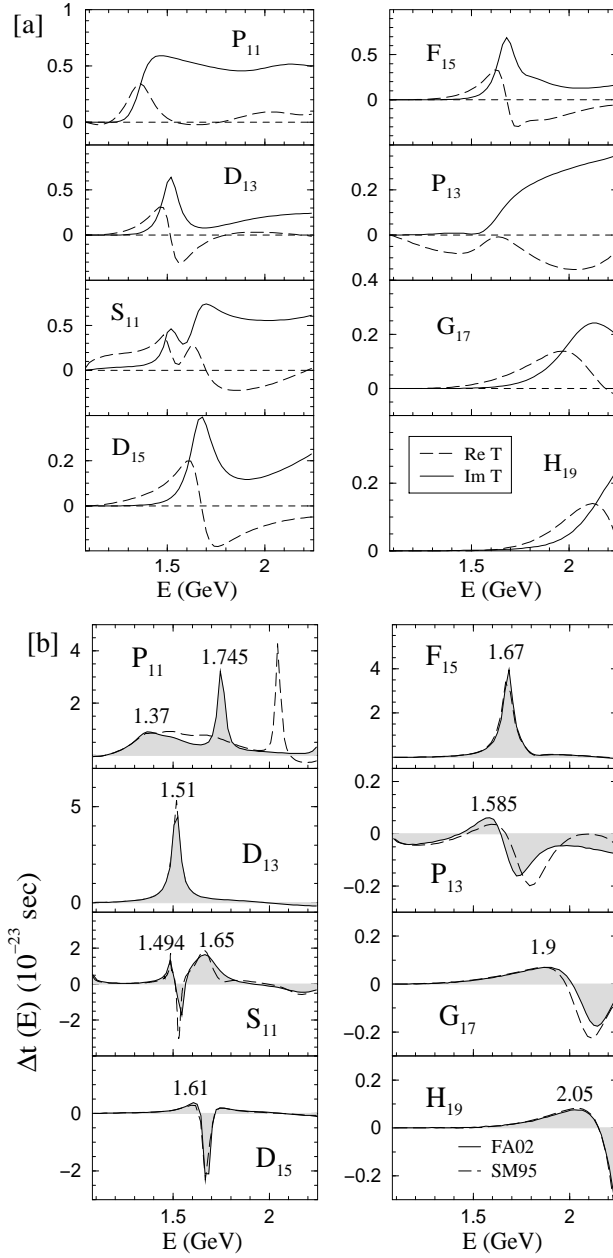


Figure 2: (a) Real (dashed lines) and imaginary (solid lines) parts of the  $T$ -matrix solutions FA02 [20] for isospin,  $I = 1/2$ , partial waves. (b) The time delay evaluated using the  $T$ -matrix solutions FA02 (shown in (a)) and an earlier version SM95 by the same group.

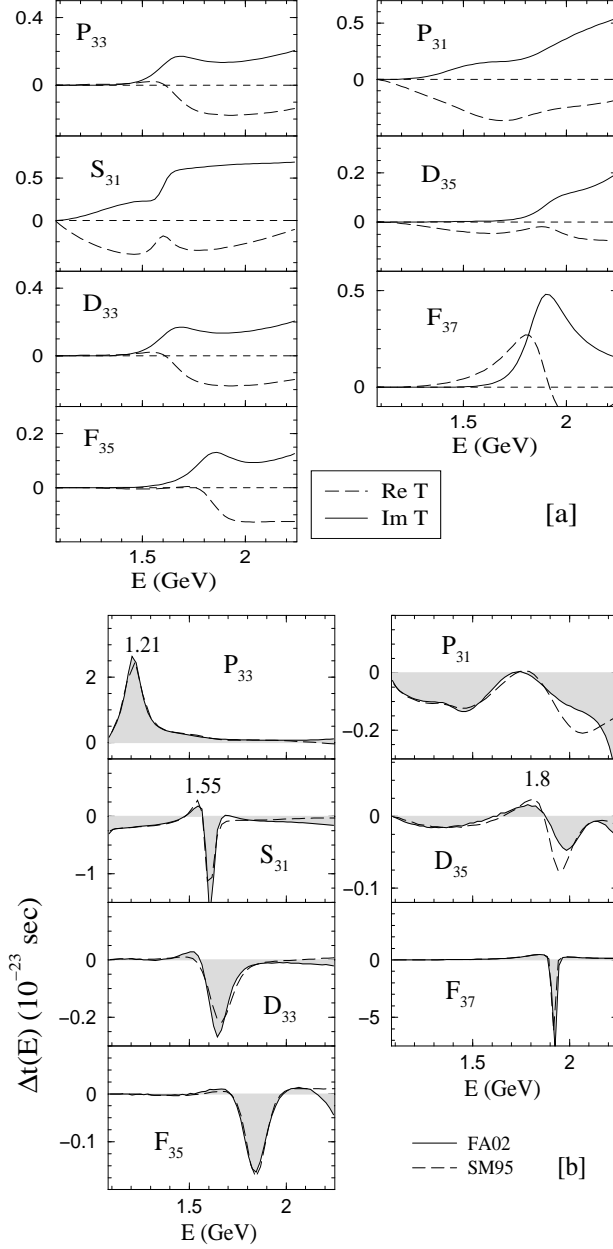


Figure 3: (a) Real (dashed lines) and imaginary (solid lines) parts of the  $T$ -matrix solutions FA02 [20] for isospin,  $I = 3/2$ , partial waves. (b) The time delay evaluated using the  $T$ -matrix solutions FA02 (shown in (a)) and an earlier version SM95 by the same group.

positions predicted by the  $T$ -matrices. However, small peaks in the  $G_{17}$  and  $H_{19}$  partial waves appear at much lower values than the poles. The shifts in the time delay peaks as compared to the pole values could be due to the presence of a non-resonant background in these partial waves. We now give a more detailed discussion for the resonances in various partial waves.

$P_{11}$ -resonances: The older solution SM95 indicates a rather broad peak around 1400 – 1500 MeV which, at the most, hints towards  $P_{11}(1440)$ . A prominent peak at  $\sim 2050$  MeV can also be found. Although this could be attributed to  $P_{11}(2100)$ , the latter is not a very well established resonance. The situation changes with the newer FA02 solution. Here the two peaks at 1370 MeV and 1745 MeV are a clear signal of  $P_{11}(1440)$  and  $P_{11}(1710)$  listed in the Summary Table. The FA02  $T$ -matrix has two closely located poles at 1357 and 1386 MeV. The broad time delay peak around 1370 could actually be due to two close overlapping resonances. The observation of the time delay peak at 1370 MeV which is much lower than the Summary Table value of 1440 MeV is similar to the finding of Ref. [21]. In fact, most of the time delay peaks being close to the pole positions, occur at lower values than the parameters of the Summary Table. The prominent peak at 2050 MeV with SM95 is not present in FA02 anymore.

$P_{13}$ -resonances: We see peaks at 1585 and 1600 MeV corresponding to the FA02 and SM95 solutions respectively. There exists a pole of the SM95 solution at 1717 MeV which is close to the resonance  $P_{13}(1720)$ . However the FA02 pole occurs at a much lower value of 1584 MeV. Though the pole values of the two solutions differ a lot, the time delay peaks with the two solutions are quite close.

$S_{11}$ -resonances: We observe a positive peak around 1494 MeV, which can be attributed to  $S_{11}(1535)$ , again as in the case of  $P_{11}(1440)$  at a considerably lower value. The positive peak at 1650 MeV is a nice manifestation of  $S_{11}(1650)$ . We would like to draw the reader's attention to another commonly found phenomena occurring in time delay plots. The small peak at 1494 MeV is followed by a large negative region (which, as emphasized before, cannot be associated with resonance formation). The negative time delay is associated with the opening up of new channels in  $\pi N$  scattering and in fact, the maximum in the dip occurs at the energy corresponding to maximum inelasticity. A detailed discussion on this issue can be found in Ref. [7]. A repulsive non-resonant background could make an additional contribution to the negative time delay.

$D_{13}$  and  $F_{15}$ -resonances: As can be seen from the figure, the peak at 1510 MeV confirms the resonance  $D_{13}(1520)$ . The time delay nicely reveals the  $F_{15}(1680)$  resonance too. The three- and two-star resonances  $D_{13}(1700)$  and  $F_{15}(2000)$  respectively, do not appear in the time delay evaluated with the SM95 or FA02 solutions. This is consistent with the fact that the same solutions do not locate the corresponding poles. However, we wish to mention here that these two resonances do appear in the time delay plots obtained from fits to the single energy values of the  $T$ -matrix which we shall discuss later.

$D_{15}$  resonance: Though the peak is not prominent, its position and width are close to the pole values.

$G_{17}$  and  $H_{19}$ -resonances: The peak positions in time delay are at much lower values as compared to the poles and much broader than the partial widths corresponding to the poles. It is not clear if such a large shift in these 2 cases should be attributed to the non-resonant background since most of the other resonances were shifted from the pole values by only few tens of MeV at most. It could be that the shifted peaks represent resonances without corresponding poles and the poles at higher values do not correspond to resonances. These cases would then be realistic examples similar to the constructed ones in Ref. [2] where the authors doubt the one-to-one correspondence between an unstable state and  $S$ -matrix pole. A good knowledge of the non-resonant background would clarify the situation.

A comparison of the time delay peaks (evaluated using the FA02 solution) with the Summary Table values and pole positions of FA02 and Speed Plots is given in Table 2. The branching fractions of the various resonances to the  $\pi N$  decay channel are also listed. The widths in time delay are the partial widths corresponding to the  $\pi N$  decay mode. Widths listed in all the other columns are full widths. It can be seen that we get distinct resonance signals even for resonances with a branching fraction as small as 10-20 % to the  $\pi N$  channel.

Next, we move on to the analysis of the  $I = 3/2$  partial waves in  $\pi N$  scattering. Many conventional pole positions of the energy-dependent  $T$ -matrices occur in regions of negative time delay. However, the time delay plots made from fits to the single energy values of the amplitude do show small peaks due to the  $\Delta$  resonances with a small branching fraction to the  $\pi N$  decay mode [7]. With the exception of  $P_{31}$  where we do not find any positive region, the overall picture is similar to the case of  $I = 1/2$  resonances.

Table 2. Comparison of nucleon resonance parameters from time delay evaluated using the FA02  $T$ -matrix solution, with the pole positions [22] of the same  $T$ -matrix, Summary Table values and Speed Plot poles ( $P = E - i\Gamma/2$ )

$L_{2I,2J}$ Mass (Full - width)	Speed Plot Pole(P) Re P [-2 Im P]	FA02 Pole (P) Re P [-2 Im P]	Branching to $\pi N$ decay mode	Time delay Peak [Partial - width]
$P_{11}^{****}$ 1440 (350)	1385 [164]	1357 [162] 1386 [170]	60 - 70 %	1370 [298] †
$D_{13}^{****}$ 1520 (120)	1510 [120]	1514 [103]	50 - 60 %	1510 [50]
$S_{11}^{****}$ 1535 (150)	1487 [110]	1516 [123]	35 - 55 %	1494 [48]
$S_{11}^{***}$ 1650 (150)	1670 [163]	1639 [155]	55 - 90 %	1650 [145]
$D_{15}^{****}$ 1675 (150)	1656 [126]	1664 [141]	40 - 50 %	1610 [93]
$F_{15}^{****}$ 1680 (130)	1673 [135]	1677 [121] 1778 [215]	60 - 70 %	1670 [75]
$D_{13}^{***}$ 1700 (100)	1700 [120]	-	5 - 15 %	-
$P_{11}^{***}$ 1710 (100)	1690 [200]	-	10 - 20 %	1745 [50]
$P_{13}^{***}$ 1720 (150)	1686 [187]	1584 [287]	10 - 20 %	1585 [124]
$P_{11}^{**}$ 2100 ( - )	-	2009 [458]	-	-
$G_{17}^{****}$ 2190 (450)	2042 [482]	2084 [453]	10 - 20 %	1900 [310]
$H_{19}^{****}$ 2220 (400)	2135 [400]	2230 [553]	10 - 20 %	2050 [276]

† Width is large due to the possibility of 2 overlapping resonances.

It is, however, fair to say that in the cases of  $D_{33}$ ,  $F_{35}$  and  $F_{37}$  partial waves, the positive peaks are really too tiny to be conclusive. A comparison of the time delay peaks in the  $I = 3/2$  partial waves (evaluated using the FA02 solution) with the Summary Table values and pole positions of FA02 and Speed Plots is given in Table 3.

Table 3. Comparison of  $\Delta$  resonance parameters from time delay evaluated using the FA02  $T$ -matrix solution, with the pole positions [22] of the same  $T$ -matrix, Summary Table values and Speed Plot poles ( $P = E - i\Gamma/2$ ).

$L_{2I,2J}$ Mass (Full - width)	Speed plots Pole (P) Re P [-2 Im P]	FA02 Pole (P) Re P [-2 Im P]	Branching to $\pi N$ decay mode	Time delay Peak [Partial - width]
$P_{33}^{****}$ 1232 (120)	1209 [100]	1211 [101]	$\geq 99$ %	1210 [108]
$P_{33}^{***}$ 1600 (350)	1550 [-]	-	10 - 25 %	-
$S_{31}^{****}$ 1620 (150)	1608 [116]	1594 [114]	20 - 30 %	1550 [54]
$D_{33}^{****}$ 1700 (300)	1651 [159]	1633 [254]	10 - 20 %	†
$S_{31}^{***}$ 1900 (200)	1780 [-]	-	10 - 30 %	-
$F_{35}^{****}$ 1905 (350)	1829 [303]	1832 [239]	5 - 15 %	†
$P_{31}^{****}$ 1910 (250)	1874 [283]	1781 [493]	15 - 30 %	-
$P_{33}^{***}$ 1920 (200)	1900 [-]	-	-	-
$D_{35}^{****}$ 1930 (350)	1850 [180]	1918 [277]	10 - 20 %	1800 [157]
$F_{37}^{****}$ 1950 (300)	1878 [230]	1871 [236]	35 - 40 %	†

† Resonance signal not very clear

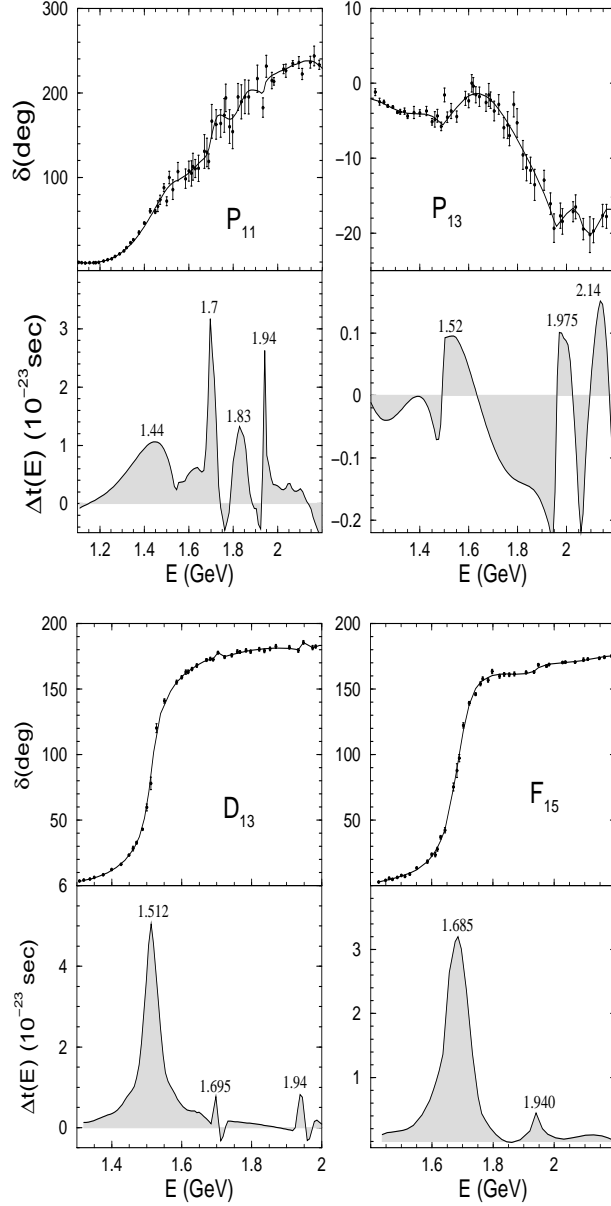


Figure 4: Single energy values of phase shifts and the corresponding time delay in the  $P_{11}$ ,  $P_{13}$ ,  $D_{13}$  and  $F_{15}$  partial waves of  $\pi N$  elastic scattering. The time delay is evaluated using the solid lines which are fits to the single energy values of phase shifts.

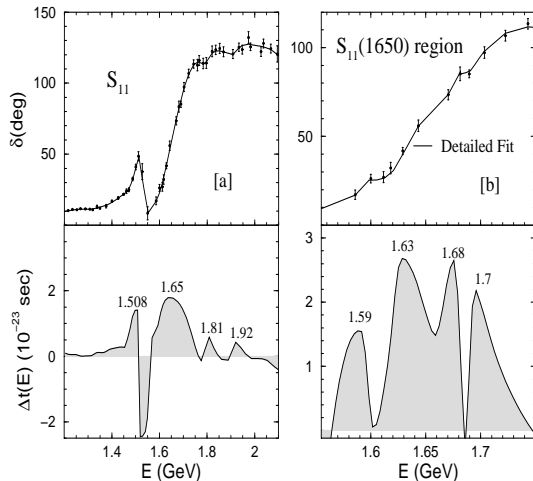


Figure 5: (a) Single energy values of phase shifts and the corresponding time delay in the  $S_{11}$  partial wave evaluated from a smooth fit to the phase shifts (b) detailed fit (solid line) to the structure in phase shift around  $E = 1650$  MeV, and the corresponding time delay.

## 5.2 Model-independent analysis and new resonances

In order to obtain model-independent lifetime plots, we shall now evaluate the time delay from fits to single energy (SE) values of phase shifts. We choose to fit SE values of phase shifts rather than the SE values of real and imaginary parts of the  $T$ -matrix, simply as a matter of convenience. The time delay evaluated using fits to phase shifts or  $T$ -matrices is actually the same. The advantage of calculating time delay from such fits is that the results are directly related to data. The disadvantage is that they are sensitive to the quality of the data and hence to the fit. We perform this analysis for the  $I = 1/2$  partial waves,  $P_{11}$ ,  $P_{13}$ ,  $D_{13}$ ,  $S_{11}$  and  $F_{15}$  in  $\pi N$  elastic scattering. It should be noted that in spite of the above mentioned disadvantage, we get strikingly similar peak positions and widths as compared to the Summary Table resonance parameters.

The results in Figs 4 and 5 reveal that the time delay has the following main characteristics: (i) it confirms well established resonances (ii) the positive peaks are now more prominent than in the case where we calculated the same quantity for the energy-dependent solutions, (iii) there exist re-

Table 4. Peak positions in lifetime and corresponding widths from model-independent time delay plots.

$L_{2I,2J}$	Summary Table Mass <sup>status</sup> [Widths]	Branching to $\pi N$ mode	Time Delay Peak [Partial Widths]
$D_{13}$	1520**** [120] 1700*** [100] 2080** [-]	50 - 60 % 5 - 15 % -	1512 [48] 1695 [12] 1940 [18]
$F_{15}$	1680**** [130] 2000** [-]	60 - 70 % -	1685 [91] 1940 [33]
$P_{11}$	1440**** [350] 1710*** [100] - 2100* [-]	60 - 70 % 10 - 20 % - -	1440 [207] 1700 [37] 1830 [65] 1940 [13]
$P_{13}$	- 1900** [-] -	- - -	1520 [101] 1975 [51] 2140 [54]
$S_{11}$	1535**** [150] - 1650**** [150] - - - 2090* [-]	35 - 55 % - 60 - 80 % - - - -	1510 [37.8] 1590 [25.2] 1630 [ $\sim$ 40] 1680 [ $\sim$ 24] 1700 [25.6] 1810 [31] 1920 [38]

gions of negative time delay in addition to the positive peaks (iv) the new feature here is that we find additional resonant peaks. At present, given the quality of the data, it is not clear if this new structure is an artifact of the fit to the data or really an indication of (new) resonances. In this context we notice that for the  $P_{11}$  and  $S_{11}$  cases the quality of the data is worse at higher energy values where indeed we have the hint for new resonances. On the other hand some one-star resonances like  $P_{11}(2100)$  and  $S_{11}(2090)$  are still not excluded. For  $F_{15}$  the quality of the data seems to be equal at low and high energy values and we find evidence for the three-star resonances  $F_{15}(2000)$  and  $P_{13}(1900)$  with some indication that the latter consists actually of two nearby resonances. In the  $D_{13}$  partial wave, we observe distinct peaks at 1512, 1695 and 1940 MeV, which could be associated with the 4-, 3- and 2-star resonances  $N(1520)$ ,  $N(1700)$  and  $N(2080)$  respectively. There also seems to be additional structure in the region 1400 – 1700 MeV in the case of  $S_{11}$ . A fit made to the detailed structure only in this region reveals the possibility of four resonances around 1650 MeV. It is interesting to note that indeed there is some support for this structure from recent works in literature [25, 26], where the existence of new resonances at 1.6 and 1.7 GeV is predicted within quark models.

With the availability of more precise data on cross sections which would enable a better extraction of the single energy values of phase shifts, one could locate the resonances from lifetime plots more accurately. We limit the discussion in this section only to the 5 partial waves shown in Figs 4 and 5 since a detailed analysis with all partial waves would make sense when the single energy values of phase shifts would be better known. We list our findings of this model-independent analysis in Table 4.

## 6 Summary

The resonances in  $\pi N$  scattering belong to the oldest subjects of particle and nuclear physics. In spite of this, the area is far from being complete as can be seen alone from the classification of baryon resonances into four-, three-, two-, and one-star resonances according to the status of being well or less established. Disagreements in the extractions of resonance parameters are often encountered and theoretical model calculations sometimes predict new resonances.

Motivated by statements in literature that a positive time delay is a necessary condition to confirm a resonance [3, 5], we have presented a systematic survey of time delay plots for the  $\pi N$  baryon resonances. The result for the time delay used here (Sec. 3) involves a total derivative of the phase shift with respect to energy. It is, however, known to be a quasiclassical approximation [23]. A more accurate expression can be seen in [24]. Because of its complicated form, we have chosen to work with the expression developed in Ref. [14].

The approach of time delay to resonances confirmed indeed the existence of many resonances. In case of a clear signal the resonance parameters can also be extracted from the time delay or lifetime plots. When  $\Delta t(E)$  was calculated from the  $T$ -matrix solutions, we did not always find these resonances at the energies corresponding to the poles of the  $T$ -matrix. We think that this is partly due to the non-resonant background as incorporated in the  $T$ -matrix solution and partly due to the fact that the  $T$ -matrix solution contains necessarily model dependent features. The calculation of  $\Delta t(E)$  directly from data via the phase shift also confirmed several established resonances. The results indicate that in some cases a known resonance state could actually be a mixture of two neighbouring resonance states. Detailed fits to the structure in the data revealed new resonances. For example, in the much talked about  $S_{11}$  partial wave [25, 26, 27] we found 4 new resonances with some of them in agreement with the predictions in literature. We believe that, given more precise data, the time delay approach to resonances is a very useful tool to extract/confirm and characterize resonances.

## References

- [1] R. H. Dalitz and R. G. Moorhouse, Proc. Roy. Soc. Lond. **A 318**, 279 (1970).
- [2] G. Calucci, L. Fonda and G. C. Ghirardi, Phys. Rev. **166**, 1719 (1968).
- [3] H. C. Ohanian and C. G. Ginsburg, Am. Journal of Phys. **42**, 310 (1974).
- [4] K. Hagiwara *et al.*, (Particle Data Group), Phys. Rev. D **66**, 010001 (2002) (URL:<http://pdg.lbl.gov>).

- [5] B. H. Bransden and R. Gordon Moorhouse, *The Pion-Nucleon System* (Princeton University Press, New Jersey, 1973); M. L. Goldberger and Watson, *Collision Theory* (John Wiley, 1964); C. J. Joachain, *Quantum Collision Theory* (North-Holland, 1975); *Quantum Mechanics*, Arno Böhm, (Springer-Verlag, 1979).
- [6] G. Höhler,  $\pi N$  Newsletter **14**, 168 (1998); *ibid*,  $\pi N$  Newsletter **9**, 1 (1993).
- [7] N. G. Kelkar, “Time advancement in resonance regions of  $\pi N$  scattering”, hep-ph/0205188.
- [8] Ken-Ichi Aoki, Atsushi Horikoshi, Etsuko Nakamura, Phys. Rev. A **62**, 22101 (2000); J. G. Muga and C. R. Leavens, Phys. Rep. **338** 353 (2000).
- [9] Z. Ahmed and S. R. Jain, “Number of quantal resonances”, (preprint 2002).
- [10] D. Bohm, *Quantum Theory* (Prentice-Hall, New York, 1951).
- [11] L. Eisenbud, dissertation, Princeton, June 1948 (unpublished).
- [12] E. P. Wigner, Phys. Rev. **98**, 145 (1955).
- [13] H. Narnhofer, Phys. Rev. D **22**, 2387 (1980).
- [14] F. T. Smith, Phys. Rev. **118**, 349 (1960).
- [15] D. M. Manley and E. M. Saleski, Phys. Rev. D **45**, 4002 (1992).
- [16] R. A. Arndt *et al.*, Phys. Rev. C **52**, 2120 (1995).
- [17] R. G. Sachs, Ann. Phys. (N.Y.) **22**, 239 (1963).
- [18] H. M. Nussenzweig, *Causality and Dispersion Relations*, Academic Press, New York and London 1972.
- [19] The values of phase shifts in different partial waves obtained by fitting the cross section data at the available energies are known as single energy (SE) values of phase shifts. The error bars on these phase shifts

naturally depend on the errors in the measured cross sections. The  $T$ -matrix is related to the phase shift and inelasticity parameter,  $\eta_l$ , as:  $T_l = (\eta_l e^{2i\delta_l} - 1)/2i$ . Thus one can also obtain SE values of the  $T$ -matrix.

- [20] Single energy values of phase shifts can be obtained from the SAID program made available on internet (URL: <http://gwdac.phys.gwu.edu>) by R. A. Arndt *et al.* To access it by telnet, link to [gwdac.phys.gwu.edu](http://gwdac.phys.gwu.edu) with ‘LOGIN:said’. Password is not required.
- [21] G. Höhler, “Against Breit-Wigner parameters- a pole-emic” D. E. Groom *et al.*, The European Physical Journal **C 15**, 1 (2000) and 1999 off-year partial update for the 2000 edition (URL: <http://pdg.lbl.gov>).
- [22] R. A. Arndt, I. I. Strakovsky *et al.*, private communication.
- [23] A. I. Baz, JETP **33**, 923 (1957).
- [24] A. I. Baz, Ya. B. Zel’dovich, A. M. Perelomov, “Scattering reactions and decay in non-relativistic quantum mechanics” (Israel Program of Scientific Translations, Jerusalem, 1969).
- [25] B. Saghai and Z. Li, nucl-th/0202007; B. Saghai and Z. Li, Eur. Phys. J. A **11**, 217 (2001).
- [26] Z. Li and R. Workman, Phys. Rev. C **53**, R549 (1996).
- [27] P. B. Siegel, S. Guertin,  $\pi N$  Newsletter **15**, 246 (1999).